Failure Analysis of a Column k-Area Fracture

By John M. Barsom and J. V. Pellegrino, Jr.

Three deep column moment connections with a Reduced Beam Section (RBS) were tested at the University of California San Diego to investigate the behavior of RBS welded moment connections (Gilton et al., 1999). One of the specimens, DC-3, had a W27×194 column, and a beam of A572 Grade 50 steel with a 5/8” thick doubler plate and 1.0” thick continuity plates. The design of specimen DC-3 is shown in Figure 1. The specimen was subjected to simulated seismic loads recommended by the SAC Joint Venture. At the peak of the second positive 4% drift cycle, specimen DC-3 developed an 8”-long crack along the k-area region of the column at the beam bottom flange level, Figure 2. The crack extended to 33” during the third positive 4% drift cycle.

The occurrence of k-area cracks in rotary straightened structural shapes has been evaluated by Tide (1999). He attributed the cracking to the low fracture toughness of the cold-worked k-area. Thus, the SAC Joint Venture sponsored the following failure analysis of specimen DC-3 to determine the cause of the fracture in the k-area.

Fractographic Analysis

A section of the column containing the crack in the k-area region was removed from specimen DC-3, Figure 2, to conduct a failure analysis of the fracture. Figure 3 is a close up of the k-area fracture at the weld access hole. It also shows the fracture of the continuity plate, which initiated at the weld access hole and propagated in a brittle manner to the free edge. Figure 4 is a close up of the fracture at the weld access hole along the weld joining the doubler plate to the column web. Also shown is the bottom end of the doubler plate, which extended 3” below the continuity plate.

The section containing the k-area crack was opened to expose the fracture surfaces, Figure 5. The chevron markings on the fracture surfaces suggested two possible initiation sites. One fracture originated from a large weld discontinuity in the weld joining the continuity plate in the column web side to the column flange, Figure 6. This crack would have fractured the continuity plate first followed by the fracture of the column web and the doubler plate weld.

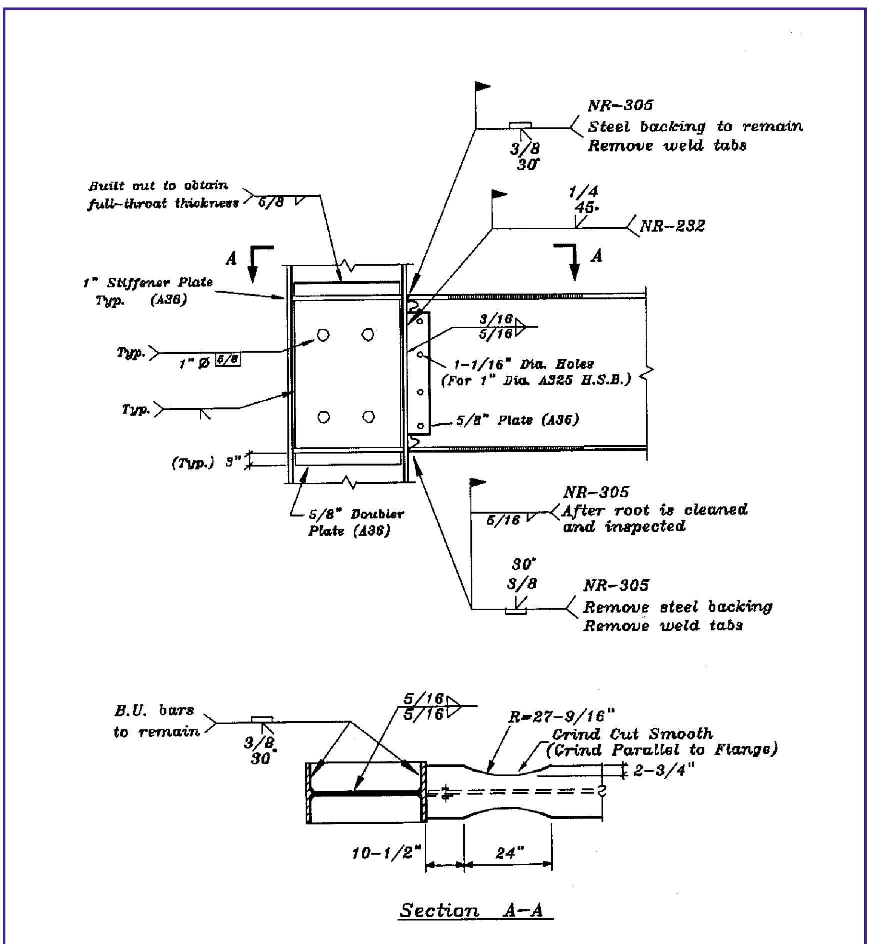

Figure 1.

The other fracture origin, Figure 7, was embedded within the column web in the vicinity of the fusion line between the doubler plate groove weld and the column web. This fracture would have severed the column web first followed by fracture of the doubler plate groove weld then the fracture of the continuity plate. Examination of the recorded strains during loading and the deformation pattern on the cracked section that was removed from the connection indicated that the 8” k-area crack occurred first, followed by the continuity plate fracture during the following positive load cycle. Therefore, the primary fracture was embedded within the column web.

Examination of the fracture surface under a light microscope and a scanning-electron microscope indicated the presence of 0.07 to 0.10” long planar inclusions (laminations) at the primary fracture origin, Figure 8, and at other locations away from the fracture origin. The sample shown in Figure 8 was tilted at a small angle to expose the laminations. The planes of these laminations were parallel to the web surfaces and perpendicular to the fracture plane. Therefore, these planes of discontinuities were parallel to the direction of stresses and strains that caused the fracture. Consequently, their contribution to the fracture process would have been negligible (Barsom and Rolfe, 1999).

Scanning-electron fractography of the fracture origin showed that the material between the two laminations at the fracture origin fractured by ductile shear then the fracture extended in a brittle cleavage mode, Figure 9. Also shown are a multitude of voids on the surface of the lamination where inclusions resided.

Metallographic examination of a transverse cross section through the fracture origin revealed the presence of laminations immediately below the fracture origin, Figure 10. These laminations contained inclusions, Figure 11, which were identified by energy-dispersive x-ray spectroscopy to be manganese silicates, Figure 12.

Figures 10 and 11 show that the ends of the laminations had extended a short distance out of plane to align themselves perpendicular to the direction of the applied stresses and strains. A high magnification scanning-electron fractograph, Figure 13, shows this extension was by formation and coalescence of ductile microvoids around inclusions and along grain boundaries. This observation demonstrates that, in the vicinity of the fracture, the steel was subjected to stress levels that approached the tensile strength prior to fracture.

Fracture Analysis

The web fracture was a single event that initiated subsurface and propagated in a brittle manner about 8” along the k-area region. Linear elastic fracture mechanics was used to establish the minimum size of an embedded crack-like imperfection that should have resided at the fracture origin had the fracture been defect governed. The relationship between fracture toughness, applied stress and the critical crack size for an embedded crack is:

$$K_{IC} = \sigma\sqrt{\frac{\pi a_c}{Q}} \qquad (1)$$

where K_{IC} = critical stress-intensity factor; σ = applied stress; a_c = critical crack size; and Q = factor related to the crack shape.

The lowest fracture toughness, K_{IC}, for any steel under the most severe conditions is equal to about 25 ksi in.$^{-1/2}$. The maximum applied stress was assumed to be equal to the tensile strength of the steel in the k-area, which was 85 ksi. Q is 2.4 for a circular penny-shaped crack and decreases to 1.0, as the crack becomes elliptical with a minor axis equal to $2a_c$ and the major axis infinite in length. Equation 1 predicts the smallest crack size when Q = 1.0.

Figure 2.

Figure 3.

Figure 4.

Figure 5.

Figure 6.

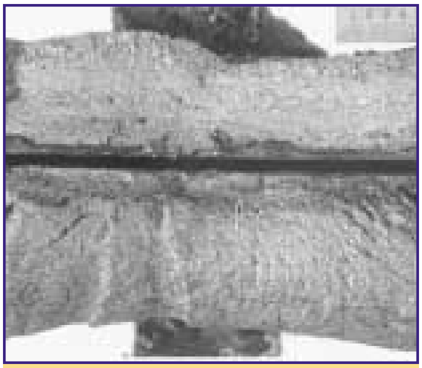

Figure 7.

Figure 8.

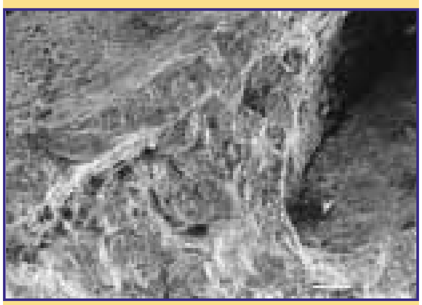

Figure 9.

Figure 10.

Figure 11.

Substituting K_{IC} = 25ksi in.$^{-1/2}$, σ = 85 ksi and Q = 1 in Eq. 1 indicates that the smallest crack size, $2a_c$, that should reside at the fracture origin is 0.056". The plane of this crack must be parallel to and on the fracture surface. The planes of the laminations were perpendicular to the fracture surface. Examination of the fracture origin did not reveal the presence of a crack-like discontinuity of any size whose plane was along the fracture surface. Therefore, the fracture was not defect governed. Also, in the absence of a crack-like imperfection at the fracture origin, the fracture is not governed by the fracture toughness of the material. The fracture exhibited all the characteristics of a tensile fracture at stresses equal to the ultimate strength of the steel under constraint conditions.

Fracture Mechanism

Gilton et al. described the behavior of specimen DC-3 under simulated seismic loads (Gilton et al., 1999). During the 4% drift cycle, an 8" long crack developed suddenly along the k-area of the column at the beam bottom flange level. Prior to fracture, the specimen exhibited significant plastic deformation of the beam flanges, beam web, column web and continuity plates. Also, the column was subjected to large out-of-plane deformation reaching 5/8" during the 4% drift cycle. Analysis of the measured strains and deformation under load indicated that specimen DC-3 was subjected to a high demand/capacity ratio at the fracture location.

The present failure analysis examined the yielding patterns on the beam flange, column flange, the panel zone and the continuity plates to identify the stresses, strains and deformations that caused the fracture. Prior to fracture, significant yielding of the beam flanges and web, the column web and continuity plate on the side of the panel zone without a doubler plate occurred at 3% drift, Figure 14 (Gilton et al., 1999). However, negligible yielding had occurred in the doubler plate or in the continuity plate attached to it.

At the instant of fracture the bottom continuity plate on the panel zone side without a doubler plate had yielded completely, Figure 3. The bottom continuity plate on the doubler plate side also yielded but to a lesser extent, Figure 4.

Extensive yielding was observed on the column flange both above and below the bottom beam flange but only on the doubler plate side of the panel zone, Figure 5. The size of the plastically deformed area was larger below than above the bottom flange. Also, yielding extended more along the edge of the column flange than along the column flange-to-web intersection, Figure 5. Negligible yielding of the column flange on the panel zone side without a doubler plate had developed at the time of the fracture, Figure 5.

The plastic deformation pattern of the column flange, Figure 5, both above and below the beam bottom flange and on both sides of the panel zone was consistent with out-of-plane bending of the column flange welded to the beam bottom flange. The larger magnitude of plastic deformation below the beam bottom flange represents the superposition of out-of-plane bending of the column flange and the bending of the beam.

The out-of-plane displacements and accompanying plastic deformation were largest at the free edge of the column flange and decreased towards the column flange mid-thickness. Thus, the outside free edge of the continuity plate increased much more than the edge that was welded to the doubler plate. The doubler plate exhibited minor plastic yielding. Therefore, the doubler plate and the column web did not increase in length beyond the elastic range. The differential displacements induced severe stress in the column web, the doubler plate and

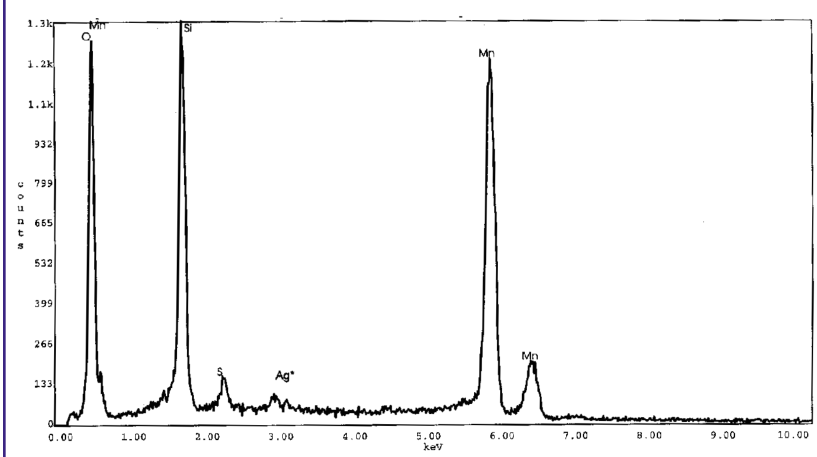

Figure 12.

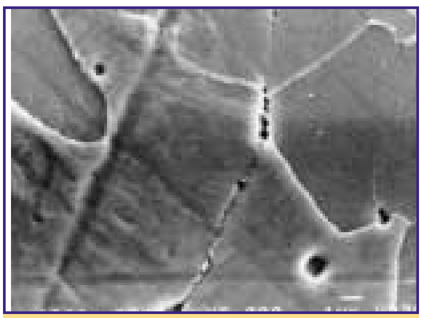

Figure 13.

Figure 14a.

Figure 14b.

the weld joining them. As the out-of-plane displacements and the beam deflection increased, the stress reached the tensile strength of the column web causing its fracture. The fracture propagated 8” along the k-area to the edge of the deformed region that was driving the crack, Figure 5. The next positive excursion extended the preexisting crack to 33” (Gilton et al., 1999).

Summary

The results of a failure analysis of a column k-area fracture may be summarized as follows:

- The k-line area origin was embedded within the web of the column;
- The fracture was not caused by pre-existing defects;
- The fracture was not influenced by the fracture toughness of the k-area region; and
- The fracture occurred when the applied stress level in the k-area region reached the tensile strength of the steel.

References

Barsom, J. M. and S. T. Rolfe. (1999) *Fracture and Fatigue Control in Structures–Applications of Fracture Mechanics*, 3rd ed., ASTM MNL41, American Society for Testing and Materials, West Conshohocken, PA.

Gilton, C. S., Brandon Chi and Chia-Ming Uang. (1999) “Brief Summary Report of Deep Column RBS Specimen DC-3”, University of California, San Diego, SAC Steel Project, SAC Joint Venture, Richmond, CA.

Tide, R. H. R. (1999) “Evaluation of steel properties and cracking in the “k”-area of W shapes.” *Engineering Structures*, 22 (2000), pp. 128-134, Elsevier Science Ltd., London, UK.

John M. Barsom is a consultant with Barsom Consulting Ltd., Pittsburgh, PA. J. V. Pellegrino, Jr., is with WHEMCO, Homestead, PA.